

## Electrostatic Double Layer Forces in the Case of Extreme Charge Regulation

Michal Borkovec\*

*Department of Inorganic, Analytical, and Applied Chemistry, University of Geneva, Sciences II,  
30 Quai Ernest-Ansermet, 1211 Geneva 4, Switzerland*

Sven H. Behrens

*School of Chemical and Biomolecular Engineering, Georgia Institute of Technology, 311 Ferst Drive,  
Atlanta, Georgia 30332-0100**Received: June 25, 2008; Revised Manuscript Received: July 23, 2008*

We analyze the interaction forces between charged surfaces across aqueous solutions under the conditions of extreme charge regulation. Under such conditions, interactions may be weaker than those given by the constant potential (CP) boundary conditions. Thermodynamically, even vanishing electrostatic interactions are conceivable. Within the constant regulation approximation, the known results can be extended to this sub-CP regime by adopting regulation parameters outside of the common range. A mean-field lattice model of an adsorbed layer shows that such conditions are most likely found near critical points within the adsorbed layer.

## 1. Introduction

Since the work of Derjaguin, Landau, Verwey, and Overbeek (DLVO),<sup>1,2</sup> interactions between two charged surfaces across aqueous solutions are routinely interpreted as a superposition of van der Waals and double layer forces.<sup>3–6</sup> This theory provides a widely used framework to analyze surface forces as measured with the surface forces apparatus (SFA) or the colloidal probe technique (see Figure 1).<sup>4–8</sup> Electrostatic double layer forces are typically estimated within the classical Poisson–Boltzmann (PB) model, or for weakly charged surfaces, within its linearized version, the Debye–Hückel (DH) theory. Comparisons with computer simulations and integral equation theories have revealed that the PB description is highly accurate for monovalent electrolytes, even up to considerable surface charge densities.<sup>9,10</sup> At short distances, however, results of the PB model depend strongly on the boundary conditions used.

Boundary conditions of constant charge (CC) and constant surface potential (CP) are popular choices because of their simplicity. In most scenarios of practical relevance, however, equilibrium with a bulk solution imposes a constant electrochemical potential of the charge-determining ions, whose adsorption at the surface regulates both the surface potential and the charge density as a function of surface separation. The simplest way to describe this situation is the constant regulation approximation (CR), which assumes a constant inner layer capacitance.<sup>11–13</sup> The resulting interaction force is widely believed to assume intermediate values between the corresponding CC value as an upper bound and the CP value as a lower bound.<sup>3–5,8,11,14</sup>

The fact that CP might not represent a lower bound to the force within the PB model was first suggested by Hall,<sup>15</sup> and subsequently, this idea was invoked repeatedly.<sup>16–18</sup> To our best knowledge, however, the interactions in this sub-CP regime were never analyzed in detail. The purpose of this letter is to explore the validity of the constant regulation (CR) approximation in this regime and to show that sub-CP behavior is most likely found near critical points and phase transitions within the adsorbed films.

## 2. Thermodynamics

Consider two planar surfaces at distance  $2L$  interacting across an indifferent excess electrolyte solution (Figure 1). For simplicity, we focus on a symmetric system composed of two identical surfaces. The specific charge  $\sigma$  per unit surface area is controlled by adsorption of a charged species (e.g., ionic surfactant), which is in equilibrium with the bulk phase. The differential of the free energy of one plate per unit area  $f(\sigma, L)$  reads at constant temperature (i.e., isothermal process)<sup>14,19</sup>

$$df = \psi d\sigma - \Pi dL \quad (1)$$

where  $\psi = (\partial f / \partial \sigma)_L$  is the conjugated electrostatic potential and  $\Pi = -(\partial f / \partial L)_\sigma$  the swelling pressure. The electrostatic potential  $\psi$  plays the role of an electrochemical potential, which controls the adsorbed amount and thus the surface charge through the bulk concentration. This potential is independent of the separation and should not be confused with the electrostatic surface potentials introduced below. Since most experiments are carried out in contact with a bulk phase (i.e., at constant  $\psi$ ), it is advantageous to consider the Legendre transform  $g(\psi, L) = f - \sigma\psi$  with the differential

$$dg = -\sigma d\psi - \Pi dL \quad (2)$$

and the corresponding relations  $\sigma = -(\partial g / \partial \psi)_L$  and  $\Pi = -(\partial g / \partial L)_\psi$ . Variations of this free energy can be measured in a force

\* To whom correspondence should be addressed. Phone: + 41 22 379 6053. Fax: + 41 22 379 6069. Email: michal.borkovec@unige.ch. Web: <http://colloid.unige.ch>.

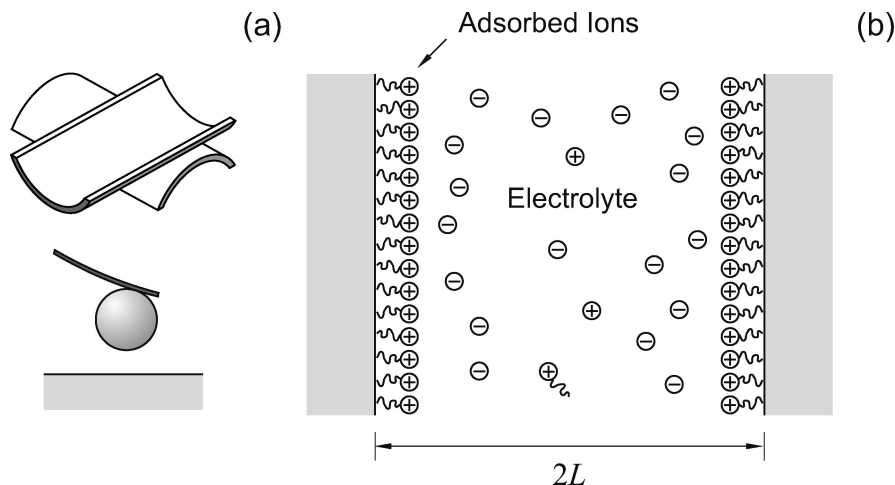


**Figure 1.** Interacting water-solid interfaces with adsorbed ions. (a) Commonly used methods to measure such interactions are the surface forces apparatus (SFA) with the crossed-cylinder geometry and the colloidal probe technique with the sphere-plane geometry based on the atomic force microscope (AFM). (b) Two planar surfaces with adsorbed charged species in equilibrium with a bulk electrolyte solution.

balance experiment. In the Derjaguin approximation,<sup>3–5,20</sup> the measured force  $F$  can be expressed as

$$F = 2\pi RW(L) \quad (3)$$

where  $R$  corresponds to the sphere radius in the sphere-plane geometry or to the cylinder radius in the crossed-cylinder geometry, and the interaction free energy  $W(L)$  per unit area is given by

$$W(L) = 2[g(\psi, L) - g(\psi, \infty)] \quad (4)$$

Taking the derivative of eq 4 with respect to  $\psi$ , one finds that the surface charge at any separation can be obtained from the surface free energy<sup>18,21</sup>

$$\sigma = \sigma_{\infty} - \frac{1}{2} \frac{\partial W}{\partial \psi} \quad (5)$$

where  $\sigma_{\infty}$  is the surface charge density for the isolated surface.

Within the present analysis, we split the free energy in two parts, namely

$$f(\sigma, L) = f_d(\sigma, L) + f_i(\sigma) \quad (6)$$

whereby the contribution of the diffuse layer  $f_d(\sigma, L)$  depends on the surface charge density  $\sigma$  and the distance  $L$ , whereas the contribution of the inner part of the double layer  $f_i(\sigma)$  depends on the surface charge density only.<sup>14</sup> As a consequence, the potential can be split as

$$\psi = \psi_d + \psi_i \quad (7)$$

where  $\psi_d$  is the diffuse layer potential and  $\psi_i$  the inner layer potential. Similarly, the total capacitance separates as

$$C^{-1} = \left( \frac{\partial \psi}{\partial \sigma} \right)_L = \left( \frac{\partial \psi_d}{\partial \sigma} \right)_L + \left( \frac{\partial \psi_i}{\partial \sigma} \right)_L = C_d^{-1} + C_i^{-1} \geq 0 \quad (8)$$

where  $C_d$  is the diffuse layer capacitance and  $C_i$  the inner layer capacitance. The inequality follows from a thermodynamic stability condition.

### 3. Diffuse Layer

Recall the free energy of the diffuse layer, which we consider in the DH approximation for simplicity.<sup>3–5</sup> The potential profile  $\phi$  within the diffuse layer is described by the DH equation

$$\frac{d^2 \phi}{dx^2} = \kappa^2 \phi \quad (9)$$

where  $\kappa$  is the inverse Debye length and  $x$  is the distance from the midplane. For a symmetric situation, the solution of eq 9 is given by  $\phi(x) = \psi_d \cosh(\kappa x) / \cosh(\kappa L)$ , and the surface charge density follows from Gauss' law

$$\sigma = \epsilon \epsilon_0 \kappa \frac{d\phi}{dx} \Big|_{x=L} = \psi_d C_{d,\infty} \tanh(\kappa L) \quad (10)$$

where the diffuse layer capacitance for the isolated wall is given by  $C_{d,\infty} = \epsilon \epsilon_0 \kappa$ . The free energy of the diffuse layer is finally obtained by considering a charging process and reads

$$f_d(\sigma, L) = \int_0^\sigma \psi_d(\sigma') d\sigma' = \frac{\sigma^2}{2C_{d,\infty}} \text{cth}(\kappa L) \quad (11)$$

### 4. Constant Regulation Approximation

The simplest way to describe the effect of the inner layer is to invoke a Taylor expansion of the free energy of the inner layer around its value at infinite separation. To second order, the free energy reads

$$f_i(\sigma) = f_i(\sigma_{\infty}) + \psi_{i,\infty}(\sigma - \sigma_{\infty}) + \frac{1}{2C_{i,\infty}}(\sigma - \sigma_{\infty})^2 \quad (12)$$

whereby the coefficients have been identified from eqs 7 and 8. Since the inner capacitance used is evaluated for the isolated surface and is taken to be constant, we refer to the constant regulation (CR) approximation. While this approximation is asymptotically exact for large separations, it often remains surprisingly accurate down to smaller separations, except very close to contact.<sup>13</sup>

The charge density for a given distance can be evaluated by taking the derivative of eq 6, inserting eqs 11 and 12, and eliminating  $\psi$  by evaluating the resulting equation for  $L \rightarrow \infty$ . The result is

$$\sigma = \sigma_{\infty} \frac{1}{p + (1-p) \text{cth}(\kappa L)} \quad (13)$$

where we have introduced the regulation parameter defined as<sup>12,13</sup>

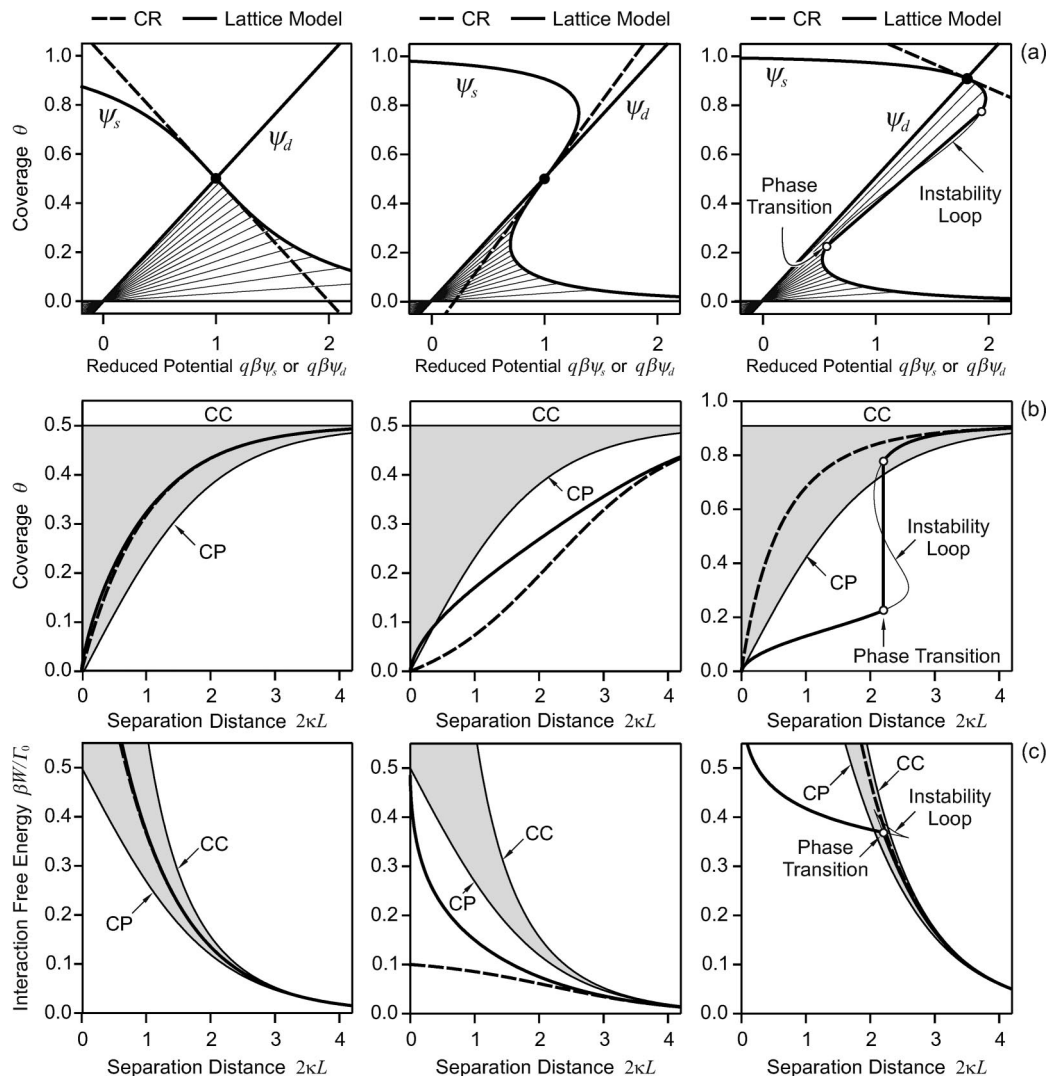


**Figure 2.** Interacting charged surfaces across an aqueous electrolyte solution described by the mean-field lattice model and constant regulation (CR) approximation. The region between constant charge (CC) and constant potential (CP) is given in gray. The adsorption equilibrium obeys a classical Langmuir isotherm (left column), a near-critical isotherm (center column), and a phase-transition case (right column). In the latter case the phase transition is indicated as  $\circ$ , and the instability loop predicted by the model is given by a thin line. The parameters are  $\alpha = -2$  and  $q\beta\psi = 0$  (left),  $\alpha = -5.6$  and  $q\beta\psi = -1.8$  (middle), and  $\alpha = -7$  and  $q\beta\psi = -2.25$  (right), and in all cases,  $\alpha' = 2$  and  $\zeta = 0$ . (a) Charge–potential plot where the isolated surface is indicated as  $\bullet$  and the situation during approach is indicated by the end point of the thin lines. The heavy line with positive slope indicates  $\psi_d$  for the isolated surface, and the thin lines passing through the origin represent the same function for smaller distances. (b) Adsorbed amount upon approach and (c) interaction free energy measured in a force balance experiment.

$$p = \frac{C_{d,\infty}}{C_{i,\infty} + C_{d,\infty}} \quad (14)$$

The CC conditions are recovered for  $p = 1$  and the CP conditions for  $p = 0$ . The free energy can be obtained by inserting eqs 11 and 12 into eq 6. The interaction free energy is then obtained from eq 4 and reads

$$W(L) = \frac{\sigma_\infty^2}{C_{d,\infty}} \cdot \frac{2e^{-2\kappa L}}{1 + (1 - 2p)e^{-2\kappa L}} \quad (15)$$

This result was first derived by Carnie and Chan.<sup>11</sup> In our notation, these authors further stated that  $0 \leq p \leq 1$ , implying that CP is a lower bound for the free energy within the model. A similar argument concerning such a lower bound has been put forward for the PB case.<sup>14</sup>

However, the notion of CP representing a lower bound must be questioned from the thermodynamic stability point of view. From eqs 8 and 14, it follows that the allowed parameter range is much larger, namely,  $-\infty < p \leq 1$ , and we refer to negative

$p$  as the sub-CP regime. For the capacitances, these conditions mean that since  $C_{d,\infty} > 0$ , the thermodynamic stability condition is not violated even if the inner layer capacitance is negative, as long it remains sufficiently small (i.e.,  $C_{i,\infty} < -C_{d,\infty}$ ). Such extreme regulation conditions were first suggested by Hall.<sup>15</sup> One finds that  $W \rightarrow 0$  as  $p \rightarrow -\infty$ .

An elegant graphical representation was introduced to visualize the effect of charge regulation.<sup>14,22</sup> One plots the diffuse layer potential  $\psi_d$  as a function of the surface charge density  $\sigma$  (cf. eq 10) and the corresponding surface potential  $\psi_s = \psi - \psi_i$ . Taking the necessary derivatives, one finds

$$\psi_s = \psi_{d,\infty} - \frac{1}{C_{i,\infty}}(\sigma - \sigma_\infty) \quad (16)$$

The equilibrium point is defined by  $\psi_s = \psi_d$  or, in other words, by eq 7. Such graphs are shown in Figure 2a. In reality, the function  $\psi_s(\sigma)$  is nonlinear, and it normally has a negative slope at the equilibrium point for an isolated surface. The CR approximation replaces this function with a straight line, which

is given by eq 16. The approximation improves with decreasing curvature of the actual function. A positive slope of this function at the equilibrium point signals the sub-CP regime and possible phase transitions.

### 5. Mean-Field Lattice Gas Model

A more realistic representation of the charging behavior of the inner layer can be made with a model describing the adsorption process. For illustration, we use a simple mean-field lattice gas model.<sup>3</sup> The model assumes that ions adsorb at well-defined adsorption sites on the surface and that they interact laterally. The free energy  $f_i(\sigma)$  of such a model can be approximated within a mean-field model as

$$\frac{\beta f_i}{\Gamma_0} = \theta \ln \theta + (1 - \theta) \ln(1 - \theta) + \frac{\alpha}{2} \theta^2 \quad (17)$$

where  $\beta = 1/(kT)$  is the inverse thermal energy,  $\Gamma_0$  the number of lattice sites per unit area,  $\alpha$  a dimensionless energy parameter, and the surface coverage  $\theta$  is related to the surface charge density via  $\sigma = q\Gamma_0\theta + \sigma_0$ , where  $q$  is the elementary charge and  $\sigma_0$  the charge density of the bare surface. For an initially uncharged surface ( $\sigma_0 = 0$ ), the variation of the charge density can be expressed as

$$\beta q \psi = \ln \frac{\theta}{1 - \theta} + [\alpha + \alpha' \operatorname{cth}(\kappa L)] \theta \quad (18)$$

where  $\alpha' = \beta q^2 \Gamma_0 (\epsilon \epsilon_0 \kappa)$ . For an isolated surface ( $L \rightarrow \infty$ ), one recovers the classical Frumkin isotherm or, equivalently, the constant capacitance model. The inner capacitance can be expressed as

$$C_{i,\infty} = \beta q^2 \Gamma_0 \frac{\theta_\infty(1 - \theta_\infty)}{1 + \theta_\infty(1 - \theta_\infty)\alpha} \quad (19)$$

where  $\theta_\infty$  is the surface coverage for the isolated surface. Indeed, the discussed sub-CP regime can be found within this model when  $\alpha$  is sufficiently negative, which signals strong attractive interactions between the adsorbed ions. The nonlinear function  $\psi_s(\sigma)$  is found from eqs 7 and 17. The corresponding CR approximation is represented with a straight line at the equilibrium point of the isolated surface (cf. eqs 16 and 19).

### 6. Illustrations

Let us now exemplify the pertinent features of the sub-PC regime. We illustrate the situation by considering surfaces that acquire charge exclusively by adsorption of cations from solution ( $\sigma_0 = 0$ ). In this case, the fractional coverage shown in Figure 2a,b is proportional to the surface charge density. We focus on this case as the more general case of an initially charged surface ( $\sigma_0 \neq 0$ ) does not reveal any new qualitative features. Figure 2b illustrates the fractional coverage as a function of the separation distance, while Figure 2c shows the interaction free energy accessible in a force balance experiment. In all cases, the mean-field lattice model is compared with the CR approximation and with the classical CC and CP solutions.

Recall first the case of a Langmuir adsorption isotherm for the isolated surface (Figure 2, left). As the surfaces approach, their charge will decrease due to charge regulation. While the CC conditions do not yield any variation in the adsorbed amount upon approach, the CP conditions predict a strong decrease. The actual decrease of the surface charge with distance lies in between CC and CP conditions and is well represented by the CR approximation ( $p = 0.5$ ), almost down to contact. The interaction energies follow a similar trend. The CC condition

results in strong repulsion, while CP results in a weaker one. The interaction in the realistic situation lies in between and is again well represented by the CR approximation. Note that a Langmuir adsorption isotherm  $\sigma(\psi)$  is obtained for charged-adsorbing species only if the lateral interactions are attractive and precisely counterbalance the repulsive interactions generated by the diffuse layer.

Let us now discuss the interesting case of a sigmoidal or supercritical isotherm (Figure 2, center). The adsorbed layer in the isolated surface lies very close to the critical point. Due to the high slope of this isotherm  $\sigma(\psi)$ , such a surface regulates extremely easily, and the charge decreases much more rapidly than that for the CP conditions ( $p = -4$ ). We refer to such extreme regulation conditions as sub-CP behavior. Again, the CR approximation remains equally valid at large distances. However, already at intermediate distances, deviations are observed. The deviations result from the substantial curvature of the isotherm. Recently, similar discrepancies between measured adsorbed amounts and the CP prediction were interpreted as a manifestation of the sub-CP behavior.<sup>17,18</sup> Corresponding trends are observed for the interaction energy (Figure 2c, center). Surprisingly, the interactions are much weaker than those predicted by the CP conditions, and at large distances, this sub-CP behavior can be well described by the simple CR approximation.

For even stronger attractive interactions within the adsorbed layer, one observes a first-order phase transition upon approach (Figure 2, right). At large distances, the CR approximation is perfectly applicable, but the behavior is very different after the system has undergone a phase transition. The phase transition is signaled by a cusp in the interaction energy. The present mean-field model predicts a triangular instability loop, where the lower corner corresponds to the locus of the first-order phase transition. The two lower edges of the instability triangle correspond to metastable branches. At its upper edge, the stability criterion is violated, and this part is thermodynamically unstable. More advanced models of adsorbed surfactant layers predict similar instability triangles upon approach.<sup>23</sup>

Evidently, the present description is highly simplified. While our predictions based on the DH approximation are bound to differ quantitatively from predictions based on the full PB model, we do not expect any qualitative differences. Near a critical point, however, an adsorbed film will undergo critical fluctuations. These fluctuations will generate lateral charge heterogeneities, which will lead to additional attractive forces.<sup>24</sup> Such lateral heterogeneities will certainly be present within a phase separation in the layer and lead to additional attractions near this point. Upon approach, such heterogeneities will influence each other, lead to rearrangements or even lead to domains undergoing charge reversal on either surface. Similar mechanisms were discussed for isolated surfaces<sup>25</sup> or for interacting surfaces on larger scales and are referred to as symmetry breaking.<sup>26</sup>

The presently proposed sub-CP conditions can probably be found experimentally. Let us mention two examples. Adsorbed films of cationic surfactants on mica are known to interact more weakly than predicted by DLVO theory with CP conditions.<sup>16–18,27,28</sup> These discrepancies have been interpreted in terms of attractive interactions resulting from lateral charge heterogeneities. While such forces are probably important in these systems, we suspect that one faces extreme regulation conditions in the sub-CP regime as well. This hypothesis is supported by the fact that adsorbed layers of cationic surfactants follow sigmoidal adsorption isotherms.<sup>29</sup> Sub-CP behavior is equally expected for



interacting weak polyelectrolyte brushes.<sup>30</sup> Hydrophobic weak polyelectrolytes may follow a sigmoidal charging curve with pH.<sup>31</sup> Near its inflection point, such a surface will again regulate very easily, leading to sub-CP behavior. Simultaneously, however, the brush will undergo a conformational transition, and presently, it is not obvious how to disentangle these two effects. Indeed, sub-CP behavior is likely to be relevant in several systems, but at the same time, it seems to be accompanied by other phenomena as well.

## 7. Conclusion

While it is often assumed that interaction forces between charged surfaces or particles in aqueous solutions are intermediate between the constant charge (CC) and the constant potential (CP) boundary conditions, the situation of weaker interactions than those given by CP conditions is investigated here. This regime is analyzed within the constant regulation (CR) approximation, where the regulation parameter  $p$  characterizes CC with  $p = 1$  and CP with  $p = 0$ . A principal result of this letter is that the sub-CP regime is thermodynamically allowed and characterized by  $p < 0$ . In the limit of  $p \rightarrow -\infty$ , the electrostatic interaction between charged surfaces vanishes entirely. As these results are based on the constant regulation (CR) approximation, they are rigorously correct only for large distances. As surfaces approach, the CR approximation becomes poorer, and this breakdown seems to happen relatively quickly in the sub-CP regime. A more detailed analysis of the interactions of charged adsorbed films within a mean-field lattice model shows that the sub-CP regime is likely found close to a critical point of the adsorbed layer (i.e., supercritical region). Below the critical point, the system may undergo a first-order phase transition upon approach. This phase transition is signaled by a cusp in the interaction energy curve. Similar situations are possibly found in adsorbed surfactant systems or polyelectrolyte brushes, but surface charge heterogeneities, surface rearrangements, or conformational transitions may complicate the naïve sub-CP picture portrayed here.

While the present discussion of the sub-CP regime is certainly relevant from the conceptual point of view, one should realize that in real systems, this regime is somewhat unusual. Charged interfaces do not regulate easily. They feature large diffuse layer capacitances and provide regulation conditions closer to CC. Observed regulation parameters are typically in the range of  $0.5 < p < 1$ , and already, situations with  $p < 0.5$  seem rare. From this point of view, already the classical CP conditions ( $p = 0$ ) must be considered as unusual, and even more so is the sub-CP regime. Nevertheless, this interesting regime appears to be more than a theoretical possibility and could be realized in several systems. At this point, however, its rigorous experimental documentation remains a challenge.

**Acknowledgment.** This work was supported by the Swiss National Science Foundation and the University of Geneva. S.H.B. gratefully acknowledges support from the Camille and Henry Dreyfus New Faculty Awards Program.

## References and Notes

- (1) Derjaguin, B.; Landau, L. D. *Acta Phys. Chim.* **1941**, *14*, 633–662.
- (2) Verwey, E. J. W.; Overbeek, J. T. G. *Theory of Stability of Lyophobic Colloids*; Elsevier: Amsterdam, The Netherlands, 1948.
- (3) Hunter, R. J. *Foundations of Colloid Science*; Oxford University Press: Oxford, U.K., 1992.
- (4) Russel, W. B.; Saville, D. A.; Schowalter, W. R. *Colloidal Dispersions*; Cambridge University Press: Cambridge, U.K., 1989.
- (5) Israelachvili, J. *Intermolecular and Surface Forces*; Academic Press: London, 1992.
- (6) Elimelech, M.; Gregory, J.; Jia, X.; Williams, R. A. *Particle Deposition and Aggregation: Measurement, Modeling, and Simulation*; Butterworth–Heinemann Ltd.: Oxford, U.K., 1995.
- (7) Ducker, W. A.; Senden, T. J.; Pashley, R. M. *Nature* **1991**, *353*, 239–241.
- (8) Butt, H. J.; Cappella, B.; Kappl, M. *Surf. Sci. Rep.* **2005**, *59*, 1–152.
- (9) Kjellander, R.; Akesson, T.; Jonsson, B.; Marcelja, S. *J. Chem. Phys.* **1992**, *97*, 1424–1431.
- (10) Guldbrand, L.; Jonsson, B.; Wennerstrom, H.; Linse, P. *J. Chem. Phys.* **1984**, *80*, 2221–2228.
- (11) Chan, D. Y. C.; Carnie, S. L. *J. Colloid Interface Sci.* **1993**, *155*, 297–312.
- (12) Behrens, S. H.; Borkovec, M. *J. Phys. Chem. B* **1999**, *103*, 2918–2928.
- (13) Pericet-Camara, R.; Papastavrou, G.; Behrens, S. H.; Borkovec, M. *J. Phys. Chem. B* **2004**, *108*, 19467–19475.
- (14) Chan, D. Y. C.; Mitchell, D. J. *J. Colloid Interface Sci.* **1983**, *95*, 193–197.
- (15) Hall, D. G. *J. Colloid Interface Sci.* **1985**, *108*, 411–413.
- (16) Yaminsky, V. V.; Ninham, B. W.; Christenson, H. K.; Pashley, R. M. *Langmuir* **1996**, *12*, 1936–1943.
- (17) Lokar, W. J.; Ducker, W. A. *Langmuir* **2002**, *18*, 3167–3175.
- (18) Subramanian, V.; Ducker, W. J. *J. Phys. Chem. B* **2001**, *105*, 1389–1402.
- (19) Podgornik, R.; Parsegian, V. A. *J. Phys. Chem.* **1995**, *99*, 9491–9496.
- (20) Bhattacharjee, S.; Elimelech, M. *J. Colloid Interface Sci.* **1997**, *193*, 273–285.
- (21) Hall, D. G. *J. Chem. Soc., Faraday Trans. 2* **1972**, *68*, 2169–2182.
- (22) Behrens, S. H.; Borkovec, M. *J. Chem. Phys.* **1999**, *111*, 382–385.
- (23) Koopal, L. K.; Leermakers, F. A. M.; Lokar, W. J.; Ducker, W. A. *Langmuir* **2005**, *21*, 10089–10095.
- (24) Miklavic, S. J.; Chan, D. Y. C.; White, L. R.; Healy, T. W. *J. Phys. Chem.* **1994**, *98*, 9022–9032.
- (25) Naydenov, A.; Pincus, P. A.; Safran, S. A. *Langmuir* **2007**, *23*, 12016–12023.
- (26) Leermakers, F. A. M.; Koopal, L. K.; Goloub, T. P.; Vermeer, A. W. P.; Kijlstra, J. *J. Phys. Chem. B* **2006**, *110*, 8756–8763.
- (27) Meyer, E. E.; Lin, Q.; Israelachvili, J. N. *Langmuir* **2005**, *21*, 256–259.
- (28) Perkin, S.; Kampf, N.; Klein, J. *Phys. Rev. Lett.* **2006**, *96*, 038301.
- (29) Goloub, T. P.; Koopal, L. K. *Langmuir* **1997**, *13*, 673–681.
- (30) Guo, X.; Ballauff, M. *Langmuir* **2000**, *16*, 8719–8726.
- (31) Garces, J. L.; Koper, G. J. M.; Borkovec, M. *J. Phys. Chem. B* **2006**, *110*, 10937–10950.

JP805595Z